A Linear Quadratic Optimal Motion Cueing Algorithm Based on Human Perception

Houshyar Asadi[1], Shady Mohamed[2], Kyle Nelson[3] and Saeid Nahavandi[4]
[1,2,3,4] Centre for Intelligent Systems Research, Deakin University
Waurn Ponds campus, VIC 3216, Australia
hasadi[1], shady.mohamed[2], kyle.nelson[3], saeid.nahavandi[4]@deakin.edu.au

Abstract

A simulator motion platform cannot exactly reproduce the longitudinal and rotational motions experienced in a real vehicle since it is constrained by its physical limits. The aim of this research is to provide a Motion Cueing Algorithm that can accurately produce vehicle accelerations and angular velocities in the simulator platform at high fidelity to give the most realistic motion, within the simulator's physical limitations. The higher order optimal washout filter based on Linear Quadratic (LQ) which takes the Vestibular system mathematical model, motion of the platform and capabilities in to account have been proposed to reduce the human perception error between simulator and real driving. Angular velocity and linear acceleration have been used in this design as the inputs for the washout filter. The obtained washout filters are the optimized transfer functions that link the simulator motion input to the vehicle motion input aiming to constrain the human sensation error and the platform motion. Thus, it overcomes the lack of human perception and conservative motion of previous classical washout filters and improves human perception, exploits available workspace more efficiently and respects physical constraints.

1 Introduction

It is physically impossible to perfectly regenerate all of the motion signals from a real vehicle in driving simulator. The reason is the motion platform workspace limitation that decreases the capabilities of replicating and regenerating rotations, accelerations and all other motions of an actual vehicle. Therefore, there is a need for a motion cueing algorithm to extract motion commands and signals from a real vehicle model and apply them to the motion platform within its workspace for reproducing simulator motion as close as possible to real vehicle motion. This is to prevent simulator sickness and platform limitations. The conventionally applied motion cueing algorithms are called washout filters and can be grouped in several categories.

Conrad and Schmidt [1, 2] presented the basic setup for the classical technique and this algorithm is largely provided as a linear cueing algorithm by Reid and Nahon [3-6]. The classical washout filter is the basic solution broadly used in different simulator types due to its simplicity and ease of adjustment [6-10]. Other advantages of classic washout algorithm include its short processing time, fast computation, stable performance and verified stability. In a six degree of freedom flight simulator study that has been conducted by Reid and Nahon [11], the classical washout filter algorithm was found to achieve good results when compared to other washout algorithms. Six degree of freedom classical washout filter algorithms were developed broadly at the University of Toronto Institute for Aerospace Studies (UTIAS) [3-5, 11-13].

The classical algorithm is composed of empirically determined high and low pass filters for the translational (in translational motion channel) and the rotational degrees of freedom (in rotational motion channel) with a crossover path that is called tilt coordination to provide the steady state or gravity alignment cues. High-pass filtering is used in the longitudinal acceleration and angular velocity resultant from vehicle dynamic model to low frequency components and extracts its transient component. A low-pass filtering can transfer the sustained part of the acceleration by tilt coordination that uses gravity as an illusory sustained acceleration. The tilt coordination must be accomplished under the driver's perception threshold which is 3.6 *deg/sec*.

Classical washout algorithms have some drawbacks. This method is very inflexible due to the fact that it demands a tuning process focused on the worst case situations, which leads to a poor usage of the workspace, the platform displacements and capabilities. As a results, this algorithm will not suit all circumstances, will produce false cues, distort the original signal and leads to wrong motion signals due to characteristics of the filters. In addition, it is difficult to simulate continuous movement with a motion platform

since the low pass filter leads to phase delay. The main disadvantage of classical washout filter algorithms is a lack of respecting human perception as vestibular system was not taken into the account in their designs and structures. The vestibular system comprises of semicircular canals and otolith organs and it is located inside the inner ear for perceiving rotational and linear motion.

Sivan, et al.[14] presented a new method called "optimal control," based on the human vestibular system. This optimal washout algorithm is based on human perception and takes into account the vestibular system model [15, 16]. Thus this method integrates a mathematical model of the human vestibular system and minimizes the sensation error between a simulated motion platform system and the actual vehicle. This new algorithm uses optimal control techniques based on linear-quadratic for developing higher order filters prior to real-time application and a cost function that depends on both sensation error between real vehicle driver and simulator driver and platform motion.

In the proposed optimal washout algorithm, the problem is to determine a washout matrix of linear transfer functions W(s) which relates the simulator motion input to the vehicle motion input to minimize the cost function by restraining both the sensation error between the simulator and vehicle driver and platform motion. The scheme of the optimal washout algorithm is illustrated in Figure 1.

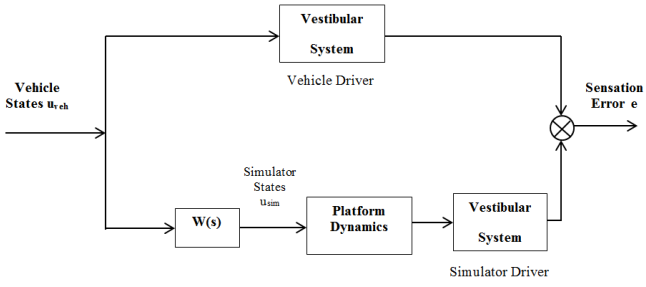

Figure 1. Linear Optimal Algorithm Problem Structure.

In earlier research, Reid and Nahon and Sivan et al. [3, 14] used linear acceleration and angular displacement as control inputs for either the longitudinal or lateral mode. Wu [17, 18] presented a technique using linear acceleration and angular acceleration for the longitudinal mode in his research. His method illustrates advantages and benefits of controlling extra motion states that do not exist in the original technique. Furthermore, as the semicircular canals act like a transducer for angular velocity input in the normal head movements range, a technique using angular velocity as input might also be preferred. Therefore, in this paper an optimal washout filter based on linear quadratic optimal control for developing higher order filters prior to real-time application will be presented. The proposed optimal is designed using linear acceleration and angular velocity as the inputs. The human perception model and platform motion are taken into account in the algorithm.

2 Optimal Washout Filter

The aim of the optimal algorithm is to calculate a transfer function W(s) that will relate the simulator motion input u_{sim} to the vehicle motion input u_{veh} as described below in equation (1)

$$u_{sim}(s) = W(s) \times u_{veh}(s) \quad (1)$$

The simulator states u_{sim} that were first considered as simulator body-axis accelerations and Euler angles [14] are then applied in order to produce the desired motion base commands. The optimal approach defines the simulator acceleration by minimizing and limiting the sensation error between the simulator and real driving as well as the linear and angular motion of the platform. The aim of this algorithm, based on its cost function is to constrain the human sensation error and the platform motion since the platform has physical workspace limitations.

In this optimal method, it is possible to find a predefined form for the solution of the optimal problem given that is formulated in a particular way. Referring to such method, the optimal gains and, thus, the desired transfer functions can be obtained by solving the Riccati equation.

Nahon and Reid [3, 12] developed an optimal motion cueing algorithm for a flight simulator based on the research that had been conducted by Sivan et al. [14]. They used the frame at the pilot's head as a center of rotation for this algorithm. Since linear filters are applied, this method works in a similar way to the classical washout algorithm. Though, the major difference is that the higher order filters and filter parameters are obtained in advance by a linear quadratic optimization process, which requires the known structure and cost function.

Figure 2 illustrates the structure of the optimal motion cueing algorithm. a_x and $\dot{\theta}$ are vehicle acceleration and angular velocity. The double integration is added in the linear path in order to change acceleration to position commands. As the algorithm uses the angular velocity as inputs, there is an integration block in the rotational path.

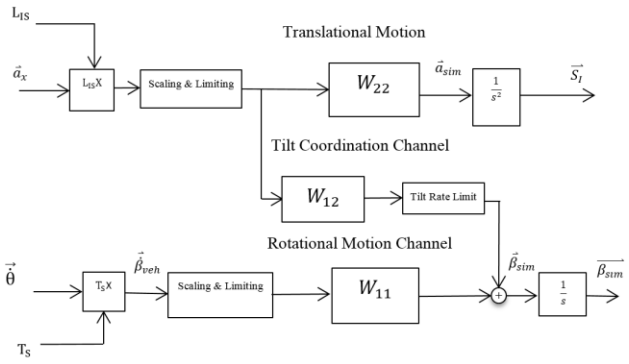

Figure 2. Optimal Algorithm block diagram for Longitudinal Mode.

2.1 Derivation of Optimal Washout Filter

The algorithm for the longitudinal (pitch/surge) mode is provided below. The input is given as

$$u = \begin{bmatrix} u_1 \\ u_2 \end{bmatrix} = \begin{bmatrix} \dot{\theta} \\ a_x \end{bmatrix} \tag{2}$$

where $\dot{\theta}$ and a_x are angular velocity and the translational acceleration respectively.

Semicircular canals can detect rotational motion sensation. Based on previous research conducted by Zacharias [15], the mathematical model of Young and Oman [19] is suitable for use as a semicircular canals model.

$$\hat{\theta} = \frac{\tau_L \tau_a s^2}{(1+\tau_a s)(1+\tau_L s)(1+\tau_S s)}\dot{\theta} \tag{3}$$

where $\hat{\theta}$ is the sensed angular velocity about each one of the three axes and τ_L, τ_S, τ_a are long time constant, short time constant and adaptation operator constant. The previous model can be rewritten as below

$$\hat{\theta} = \frac{T_3 s^2}{s^3 + T_2 s^2 + T_1 s + T_0}\dot{\theta} \tag{4}$$

where

$$T_0 = \frac{1}{\tau_a \tau_L \tau_S} \tag{5}$$

$$T_1 = \frac{\tau_a + \tau_L + \tau_S}{\tau_a \tau_L \tau_S}$$

$$T_2 = \frac{\tau_L \tau_S + \tau_a \tau_L + \tau_a \tau_S}{\tau_a \tau_L \tau_S}$$

$$T_3 = \frac{\tau_a \tau_L}{\tau_a \tau_L \tau_S}$$

The previous transfer function can be expressed in state space as

$$\dot{x}_{SCC} = A_{SCC} x_{SCC} + B_{SCC} u \tag{6}$$

$$\hat{\theta} = C_{SCC} x_{SCC} + D_{SCC} u$$

and its canonical observer form is

$$A_{SCC} = \begin{bmatrix} -T_2 & 1 & 0 \\ -T_1 & 0 & 1 \\ -T_0 & 0 & 0 \end{bmatrix} \tag{7}$$

$$B_{SCC} = \begin{bmatrix} T_3 & 0 \\ 0 & 0 \\ 0 & 0 \end{bmatrix}$$

$$C_{SCC} = [1 \quad 0 \quad 0]$$

$$D_{SCC} = [0 \quad 0]$$

Otolith organs are responsible for perceiving linear motion in the head. Young and Meiry [20] provided a modified model for sensing linear acceleration that can solve this, and sense tilt based on summarization of references [15, 21]

$$\hat{f}_x = K'_{OTO} \frac{(s + A_0)}{(s + B_0)(s + B_1)} f_x(s) \tag{8}$$

where f is the stimulus specific force and $\hat{f}$ is sensed specific force along each one of the three axes. K'_{OTO}, B_0, B_1 and A_0 are defined as computed parameters for a static sensitivity, long time constant, short time constant and lead operator.

For the center of rotation at the centroid of the driver's head, the specific force is

$$f_x = a_x + g\theta \tag{9}$$

The previous equation can be transformed into the Laplace domain as below

$$f_x(s) = u_2(s) + \left(g\frac{1}{s}\right)u_1(s) \tag{10}$$

Substituting (10) into (8) results in equation (11) as below

$$\hat{f}_x(s) = K'_{OTO}\frac{(s + A_0)}{(s + B_0)(s + B_1)}\left[u_2(s) + \left(g\frac{1}{s}\right)u_1(s)\right] = \tag{11}$$

$$G_{OTO}K'_{OTO}\frac{(s + A_0)}{(s + B_0)(s + B_1)}\left[\left(g\frac{1}{s}\right) \quad 1\right]u =$$

$$G_{OTO}K'_{OTO}\left[\frac{gs + gA_0}{s(s + B_0)(s + B_1)} \quad \frac{(s + A_0)}{(s + B_0)(s + B_1)}\right]u$$

Rearranging the previous equation results in the following differential equation

$$\ddot{\hat{f}}_x + (B_0 + B_1)\dot{\hat{f}}_x + B_0 B_1 \hat{f}_x = K'_{OTO}[g.u_1 + g.A_0 \int u_1\, dt + \dot{u}_2 + A_0 u_2] \tag{12}$$

The equation (12) can be rewritten as below

$$\dddot{\hat{f}}_x + a\ddot{\hat{f}}_x + b\dot{\hat{f}}_x = c\dot{u}_1 + du_1 + e\int u_1\, dt + f\dot{u}_2 + hu_2 \tag{13}$$

and also can be shown in state space as

$$\dot{x}_{OTO} = A_{OTO} x_{OTO} + B_{OTO} u \tag{14}$$

$$\hat{f}_x = C_{OTO} x_{OTO} + D_{OTO} u$$

where x_{OTO} and u are the otoliths states and input of the system respectively, and A_{OTO}, B_{OTO}, C_{OTO} and D_{OTO} are given as

$$A_{OTO} = \begin{bmatrix} 0 & 1 & 0 & 0 & 0 \\ -b & -a & 1 & 0 & 0 \\ 0 & 0 & 0 & 0 & 0 \\ 0 & 0 & 0 & 0 & 1 \\ 0 & 0 & 0 & -b & -a \end{bmatrix} \quad (15)$$

$$B_{OTO} = \begin{bmatrix} c & 0 \\ d - ac & 0 \\ e & 0 \\ 0 & f \\ 0 & h - af \end{bmatrix}$$

$$C_{OTO} = [1 \quad 0 \quad 0 \quad 1 \quad 0]$$

$$D_{OTO} = [0 \quad 0]$$

The total state space representation of the vestibular system consisting of semicircular canal and otolith models can be represented for the human vestibular model as

$$\dot{x}_V = A_V x_V + B_V u \quad (16)$$

$$\hat{y}_1 = C_V x_V + D_V u$$

where x_V is the total human vestibular model states and $\hat{y}_1$ is the sensed responses. Also A_V, B_V, C_V, and D_V show the total vestibular models as one set of state equations

$$A_V = \begin{bmatrix} A_{SCC} & 0 \\ 0 & A_{OTO} \end{bmatrix} \quad (17)$$

$$B_V = \begin{bmatrix} B_{SCC} \\ B_{OTO} \end{bmatrix}$$

$$C_V = \begin{bmatrix} C_{SCC} & 0 \\ 0 & C_{OTO} \end{bmatrix}$$

$$D_V = \begin{bmatrix} D_{SCC} \\ D_{OTO} \end{bmatrix}$$

It is assumed that the same perception model is applied to both the driver in the vehicle and simulator as shown in Figure 1.

Thus, in this case the vestibular state error is given as $x_e = x_{sim} - x_{veh}$ where x_{sim} is the vestibular states for simulator driver and x_{veh} are the vestibular states for vehicle driver. The driver sensation error e is

$$\dot{x}_e = A_V x_e + B_V u_{sim} - B_V u_{veh} \quad (18)$$

$$e = C_V x_e + D_V u_{sim} - D_V u_{veh}$$

where u_{sim} and u_{veh} show the simulator and vehicle inputs as given in equation (2).

Since the simulator has limitations, the simulator motion should be constrained. Therefore, the control algorithm must take the linear velocity, displacement and integral displacement of the simulator as well as angular rotation into account in the cost function. To this end, the following additional terms of simulator x_d are involved in the state equations

$$\dot{x}_d = A_d x_d + B_d u_{sim} \quad (19)$$

$$x_d = \begin{bmatrix} \iiint a_x \, dt^3 & \iint a_x \, dt^2 & \int a_x \, dt & \theta \end{bmatrix}^T$$

and is linked to the simulator input u_{sim} by

$$A_d = \begin{bmatrix} 0 & 1 & 0 & 0 \\ 0 & 0 & 1 & 0 \\ 0 & 0 & 0 & 0 \\ 0 & 0 & 0 & 0 \end{bmatrix} \quad (20)$$

$$B_d = \begin{bmatrix} 0 & 0 \\ 0 & 0 \\ 0 & 1 \\ 1 & 0 \end{bmatrix}$$

As recommended in Sivan's research, filtered white noise can be used as an input to this system with the purpose of regenerating several driving situations. This indicates that an additional state space model is added to one created earlier, whose states are the input. The optimal algorithm that has been provided designs an optimal scheme and a set of optimal parameters subject to the presumptions of workspace limitation and human vestibular models by solving the Riccati equation.

The vehicle input u_{veh} consists of filtered white noise, and can be stated as below

$$\dot{x}_n = A_n x_n + B_n w \quad (21)$$

$$u_{veh} = x_n$$

In the previous equation x_n are the filtered white noise states and w shows white noise. A_n and B_n are given as

$$A_n = \begin{bmatrix} -\gamma_1 & 0 \\ 0 & -\gamma_2 \end{bmatrix} \quad (22)$$

$$B_n = \begin{bmatrix} \gamma_1 \\ \gamma_2 \end{bmatrix}$$

where γ_1 and γ_2 are the first-order filter break frequencies for each degree-of-freedom. The state equations (18), (19) and (21) can be combined to form the preferred system equation as below

$$\dot{x} = Ax + B u_{sim} + Hw \quad (23)$$

$$y = [e \quad x_d]^T = Cx + Du_{sim}$$

where y is defined as the desired output, and $x = [x_e \quad x_d \quad x_n]^T$ shows the combined states. The combined system matrices A, B, C, D, and H are then presented by

$$A = \begin{bmatrix} A_V & 0 & -B_V \\ 0 & A_d & 0 \\ 0 & 0 & A_n \end{bmatrix} \quad (24)$$

$$B = \begin{bmatrix} B_V \\ B_d \\ 0 \end{bmatrix}$$

$$H = \begin{bmatrix} 0 \\ 0 \\ B_n \end{bmatrix}$$

$$C = \begin{bmatrix} C_V & 0 & -D_V \\ 0 & I & 0 \end{bmatrix}$$

$$D = \begin{bmatrix} D_V \\ 0 \end{bmatrix}$$

The cost function for the optimal motion cueing algorithm J is specified as

$$J = E\{\int_{t_0}^{t_1} (e^T Q e + x_d^T R_d x_d + u_{sim}^T R u_{sim}) dt\} \quad (25)$$

where E{ } is the mathematical mean of statistical variable (average or expected value), Q and R_d are positive semi definite matrices, and R is a positive definite matrix. The above equation indicates that there are three variables to be restrained and limited in the cost function. These variables are the sensation error e and also extra terms such as x_d and u_{sim} which together describe the linear and angular motion of the platform in the proposed cost function. Thus, x_d is the state vector or platform position and velocity, and u_{sim} is the platform longitudinal acceleration in the cost function. The purpose of the algorithm based on its cost function is to constrain the human sensation error and the platform motion due to physical workspace limitations.

The system equation and cost function can be converted to the standard optimal control form [22] as shown in following equations

$$\dot{x} = A'x + B\,u' + Hw \quad (26)$$

$$J' = E\{\int_{t_0}^{t_1} (x^T R_1' x + u'^T R_2 u') dt\}$$

where

$$A' = A - BR_2^{-1}R_{12}^T,\ u' = u_S + R_2^{-1}R_{12}^T x,\ R_1' = R_1 - R_{12}R_2^{-1}R_{12}^T \quad (27)$$

$$R_1 = C^T G C,\ R_{12} = C^T G D,\ R_2 = R + D^T G D,\ G = \mathrm{diag}[Q, R_d]$$

The cost function of equation (26) is minimized when

$$u' = -R_2^{-1}B^T P x \quad (28)$$

P is the solution of the following algebraic Riccati equation

$$R_1' - PBR_2^{-1}B^T P + A'^T P + PA' = 0 \quad (29)$$

By substituting equation (28) into (27) and solving for u_{sim},

$$u_{sim} = -[R_2^{-1}(B^T P + R_{12}^T)]x \quad (30)$$

and specifying a matrix K, where $u_{sim} = -Kx$, leads to equation (31) as given below

$$K = R_2^{-1}(B^T P + R_{12}^T) \quad (31)$$

where K can be subdivided resultant to the partition of x state in given equation

$$u_{sim} = -[K_1 \quad K_2 \quad K_3]\begin{bmatrix} x_e \\ x_d \\ x_n \end{bmatrix} \quad (32)$$

As $x_n = u_A$, we eliminate the states corresponding to x_n from equation

$$\begin{bmatrix} \dot{x}_e \\ \dot{x}_d \end{bmatrix} = \begin{bmatrix} A_V & 0 & -B_V \\ 0 & A_d & 0 \end{bmatrix}\begin{bmatrix} x_e \\ x_d \\ u_{veh} \end{bmatrix} + \begin{bmatrix} B_V \\ B_d \end{bmatrix} u_{sim} \quad (33)$$

Substituting equation (32) into (33) and recalculating them results in the following equation

$$\begin{bmatrix} \dot{x}_e \\ \dot{x}_d \end{bmatrix} = \begin{bmatrix} A_V - B_V K_1 & -B_V K_2 \\ -B_d K_1 & A_d - B_d K_2 \end{bmatrix}\begin{bmatrix} x_e \\ x_d \end{bmatrix} + \begin{bmatrix} -B_V(I + K_3) \\ -B_d K_3 \end{bmatrix} u_{veh} \quad (34)$$

After noting the state space form of equation (34) and (18) the subsequent equations are obtained in the Laplace domain

$$u_{sim}(s) = W(s) \times u_{veh}(s) \quad (35)$$

$$W(s) = [K_1 \quad K_2]\begin{bmatrix} sI - A_V + B_V K_1 & B_V K_2 \\ B_d K_1 & sI - A_d + B_d K_2 \end{bmatrix}^{-1}\begin{bmatrix} B_V(I + K_3) \\ B_d K_3 \end{bmatrix} - K_3$$

W(s) is a matrix of the optimized transfer functions that link the simulator motion input u_{sim} to the vehicle motion input u_{veh}. The block diagram for the on-line optimal algorithm structure is given in Figure 2.

3 Simulation and Results

3.1 Driving scenario

In order to evaluate the proposed motion cueing algorithm, data was recorded during a virtual driving scenario.

The vehicle simulation environment utilized for this experiment is based on the Rigs of Rods [23] soft body physics engine (version 0.39.5). This open source software was modified to enable adjustment of the driver's position, head tracking capability and integration of haptic vehicle controls. The software was also modified to enable key vehicle data to be presented on a heads-up display, saved to a file for later analysis and exported in real time to a motion platform. Data being extracted included the vehicle

position, velocity, acceleration, orientation, angular velocity, angular acceleration, RPM and gear, as well as driver input such as steering, throttle, brake and clutch, the driver's head position and orientation, and the terrain data at each wheel location.

The vehicle simulation software has been customized to enable integration with the haptically-enabled Universal Motion Simulator (UMS) [24] developed by the Centre for Intelligent Systems Research (CISR) at Deakin University. The UMS represents the next generation of vehicle simulation, featuring a far greater range of motion, greater flexibility and more realism. The state-of-the-art UMS system is based on a highly customized 6-degree-of-freedom serial robot which features a large motion envelope, high-resolution kinematic control, two-axes of continuous rotation and realistic acceleration. This introduces capability for maneuvers that cannot be replicated by Stewart platforms and enables simulation of even the most unusual vehicle motion including response to varying terrain and weather conditions, large tilt angles, large vertical displacements, slipping and rollover. The UMS is the ultimate human-machine interface (HMI) enabling complete immersion in the simulation environment through the integration of haptic vehicle controls, an immersive high-resolution 3D capable head-mounted display, head tracking capability and a complete 36 camera motion capture and tracking system. The modular UMS design supports realistic driver training for multiple vehicle types in a controlled, safe and low-cost environment.

Experiments were conducted with the proposed algorithm across a range of terrain types and driving scenarios. The results below are derived from data recorded from the "Outback" [25] terrain. This environment was selected as it features a wide range of driving scenarios such as rapid acceleration and deceleration, uphill and downhill sections, banked sections, flat sections, sections with uneven road surface, left and right turns, hairpin type turns and straighter sections. Figure 3 depicts a bird's eye view of the track; the driving path of the vehicle during the scenario is shown in red. The vehicle utilized during experimentation was the Hummer H1.

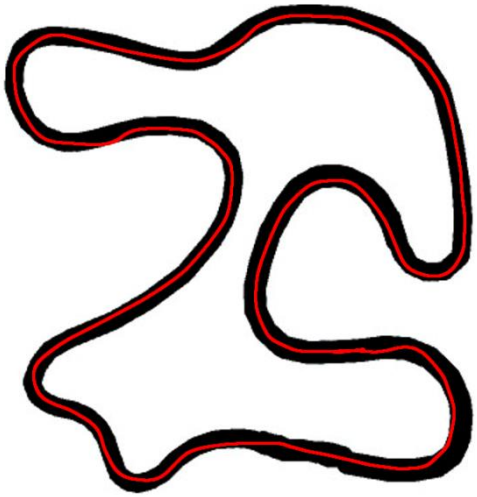

Figure 3. Aerial perspective of the "Outback" track including the vehicle path during the driving scenario.

3.2 Results

The proposed optimal motion cueing algorithm was implemented in MATLAB/Simulink. The results of the optimal motion cueing algorithm present an optimal washout matrix of the optimized transfer functions that link the simulator motion input to the vehicle motion input linear (surge acceleration and pitch angular velocity). In this case, four transfer function matrices from the two inputs (the vehicle accelerations and Euler angles) to the two outputs which are the simulator body-axis translational accelerations and the rotational angles are computed. The obtained washout filter matrix and its transfer functions are given as below

$$W(s) = \begin{bmatrix} W_{11}(s) & W_{12}(s) \\ W_{21}(s) & W_{22}(s) \end{bmatrix} \tag{36}$$

$$W_{11} = \frac{2.173\ s^8 + 1015\ s^7 + 5.027e04\ s^6 + 3.357e05\ s^5 + 9.422e05\ s\text{^}4 + 1.421e06\ s\text{^}3 + 1.201e06\ s\text{^}2 + 4.759e05\ s + 2.977e04}{s^8 + 720.5\ s^7 + 3.831e04\ s^6 + 3.237e05\ s^5 + 9.587e05\ s^4 + 1.44e06\ s\text{^}3 + 1.214e06\ s\text{^}2 + 4.802e05\ s + 3.025e04}$$

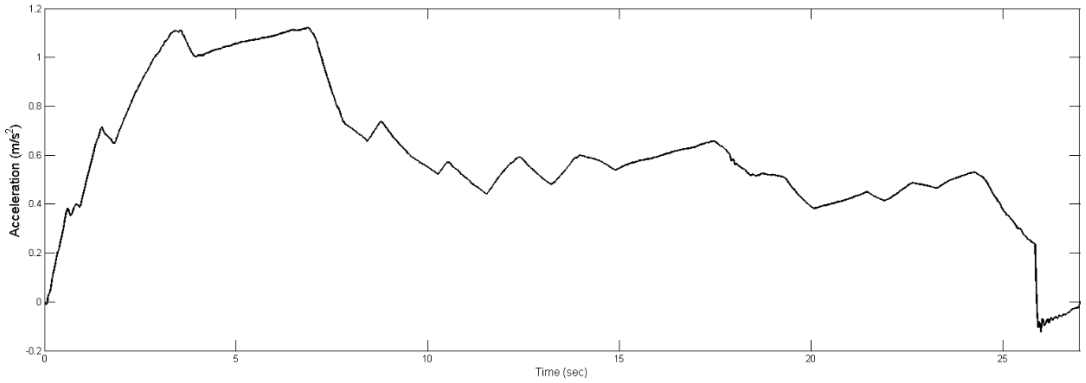

Figure 4. Recorded reference acceleration for surge mode

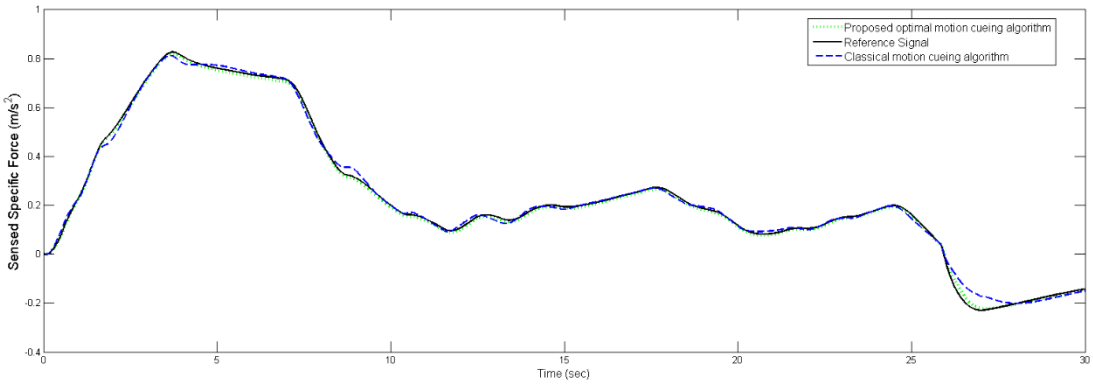

Figure 5. Longitudinal sensed specific force of reference, proposed optimal and classical motion cueing algorithm

$$W_{12} = \frac{1.378\ s^8 + 349.3\ s^7 + 1.514e04\ s^6 + 7.668e04\ s^5 + 1.428e05\ s\text{^}4 + 1.218e05\ s\text{^}3 + 4.823e04\ s\text{^}2 + 3001\ s}{s^8 + 720.5\ s^7 + 3.831e04\ s^6 + 3.237e05\ s^5 + 9.587e05\ s^4 + 1.44e06\ s\text{^}3 + 1.214e06\ s\text{^}2 + 4.802e05\ s + 3.025e04}$$

$$W_{21} = \frac{-0.9981\ s^8 - 678.3\ s^7 - 1.087e04\ s^6 - 1.566e05\ s^5 - 2.235e05\ s\text{^}4 - 1.619e04\ s\text{^}3 - 0.3039\ s\text{^}2}{s^8 + 720.5\ s^7 + 3.831e04\ s^6 + 3.237e05\ s^5 + 9.587e05\ s^4 + 1.44e06\ s\text{^}3 + 1.214e06\ s\text{^}2 + 4.802e05\ s + 3.025e04}$$

$$W_{22} = \frac{0.6877\ s^8 + 504.4\ s^7 + 3.206e04\ s^6 + 1.241e05\ s\text{^}5 + 3.113e04\ s\text{^}4 + 1669\ s\text{^}3}{s^8 + 719.2\ s^7 + 3.737e04\ s^6 + 2.749e05\ s^5 + 6.074e05\ s^4 + 7.098e05\ s\text{^}3 + 4.208e05\ s\text{^}2 + 7.804e04\ s + 3805}$$

The recorded reference signal according to section 3.1 is shown in Figure 4. Both the proposed optimal and classical washout filter are compared using real recorded input with a duration of 27 seconds.

The primary of the optimal method is better tracking of the reference sensed signal (real vehicle) and reducing human perception error between real and simulator driver within the physical limitations. Figure 5 shows longitudinal sensed specific force of reference, for the proposed optimal and classical motion cueing algorithm. According to this figure the output result of proposed optimal motion cueing algorithm is following the reference signal more accurately compared to the classical washout filter since the human vestibular sensation is taken into account in this algorithm. The classical sensed specific result is fluctuated near of reference signal that shows inconsistency of previous method.

The longitudinal perceived specific force error of the proposed optimal and classical motion cueing algorithm between the real and simulator driver is shown in Figure 6. It is illustrated that the human sensation error has been reduced compared to the classical washout filter. This improvement in human sensation leads to reduction and elimination of simulator sickness.

Translational platform displacement using the proposed optimal and classical motion cueing algorithm is shown in Figure 7. As illustrated, the classical algorithm is conservative in using physical workspace while the optimal motion cueing algorithm exploits the physical limitations more efficiently to reduce the human perception error. This is due to the consideration of human perception and inclusion of linear and angular motion of the platform in the algorithm cost function. Also, as shown in Figure 8, the optimal motion cueing algorithm angular velocity does not exceed from the human rotational threshold that is 3.6 *deg/sec*. Therefore, the surge motion cannot be perceived as a rotational false motion cue. The RMS (Root Mean Square) error of sensed specific force is decreased from 0.0118 m/sec^2 to 0.0079 m/sec^2 by utilizing the proposed optimal washout filter method instead of classical washout filter. The cross correlation coefficients between the output sensation result and reference signal in classical washout filter is 0.9985 which is increased to 0.9999 in the proposed optimal washout filtering method. It shows the optimal algorithm has followed the motion reference more satisfactorily.

4 Conclusion

The optimal motion cueing algorithm presented aims to overcome the shortcomings of the classical washout algorithm such as false motion, phase delay and, lack of human perception and conservative motion features that leads to poor usage of simulator workspace. The algorithm takes the human perception model and simulator motion states and capabilities into account. This is to constrain the human sensation error and the platform motion due to physical workspace limitations. This algorithm is based on Linear Quadratic (LQ) and angular velocity and translational acceleration to minimize the human perception error between simulator and real driver. The proposed optimal motion cueing algorithm is implemented in the MATLAB/Simulink software packages. The performance of the proposed optimal algorithm is compared with the classical algorithm. The RMS error of sensed specific force is reduced and correlation coefficients are increased between simulated and real driver compared to previous method. The presented results show the capability of this method over classical method due to its better performance, high fidelity motions, improved human sensation and exploiting the platform more efficiently within the simulator's physical limitations. Also the produced signal can follow the reference signal more accurately compared to classical washout filtering strategy.

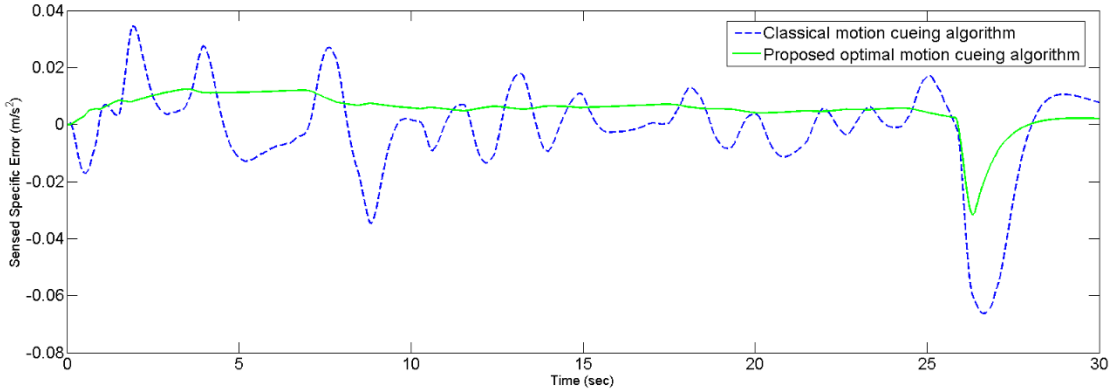

Figure 6. Longitudinal sensed specific force error comparison of proposed optimal and classical motion cueing algorithm

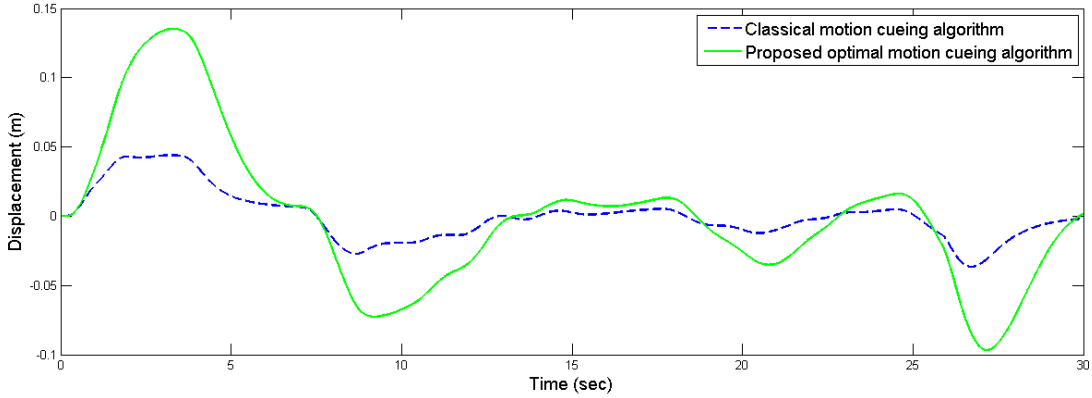

Figure 7. Translational workspace displacement comparison of proposed optimal and classical motion cueing algorithm

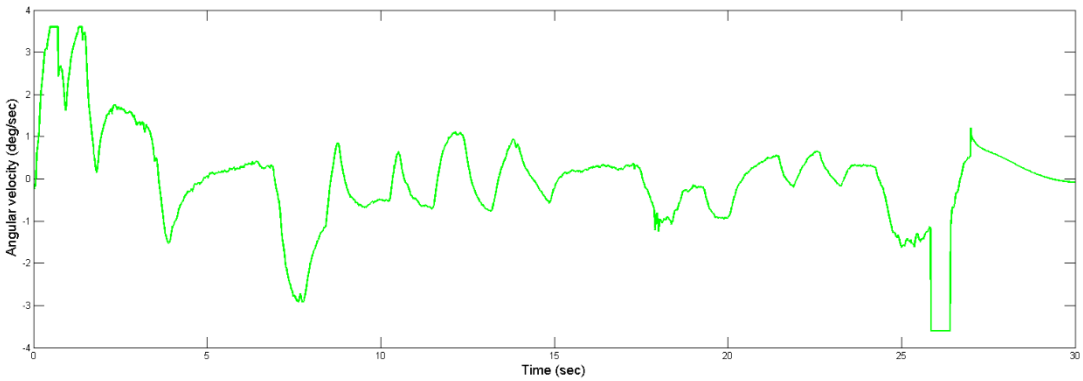

Figure 8. Optimal motion cueing algorithm angular velocity

References

[1] B. Conrad and S. Schmidt, "A study of techniques for calculating motion drive signals for flight simulators," *NASA CR-114345*, 1971.

[2] B. Conrad, S. Schmidt, and J. Douvillier, "Washout circuit design for multi-degrees of freedom moving base simulators," in *Proceedings of the AiAA Visual and Motion Simulation Conference, Palo Alto (CA), September 10*, 1973.

[3] L. Reid and M. Nahon, *Flight Simulation Motion-base Drive Algorithimns: Part 1-Developing and Testing the Equations*: Institute for Aerospace Studies, Toronto University, 1985.

[4] L. Reid and M. A. Nahon, "Flight Simulation Motion-Base Drive Algorithms.: Part 2, Selecting The System Parameters," *Utias Report*, 1986.

[5] L. Reid and M. Nahon, "Flight simulation motion-

base drive algorithms. Part 3: Pilot evaluations," 1986.

[6] L. Nehaoua, H. Mohellebi, A. Amouri, H. Arioui, S. Espié, and A. Kheddar, "Design and control of a small-clearance driving simulator," *Vehicular Technology, IEEE Transactions on*, vol. 57, pp. 736-746, 2008.

[7] L. Nehaoua, A. Amouri, and H. Arioui, "Classic and adaptive washout comparison for a low cost driving simulator," in *Intelligent Control, 2005. Proceedings of the 2005 IEEE International Symposium on, Mediterrean Conference on Control and Automation*, 2005, pp. 586-591.

[8] L. Nehaoua, H. Arioui, H. Mohellebi, and S. Espie, "Restitution movement for a low cost driving simulator," in *American Control Conference, 2006*, 2006, p. 6 pp.

[9] H. Asadi, A. Mohammadi, S. Mohamed, D. Rahim Zadeh, and S. Nahavandi, "Adaptive Washout Algorithm Based Fuzzy Tuning for Improving Human Perception," in *Neural Information Processing: 21st International Conference, ICONIP 2014, Kuching, Malaysia, November 3-6, 2014. Proceedings, Part III*, 2014, pp. 483-492.

[10] H. Asadi, A. Mohammadi, S. Mohamed, and S. Nahavandi, "Adaptive Translational Cueing Motion Algorithm Using Fuzzy Based Tilt Coordination," in *Neural Information Processing*, 2014, pp. 474-482.

[11] L. D. Reid and M. A. Nahon, "Response of airline pilots to variations in flight simulator motion algorithms," *Journal of Aircraft*, vol. 25, pp. 639-646, 1988.

[12] M. A. Nahon and L. D. Reid, "Simulator motion-drive algorithms-A designer's perspective," *Journal of Guidance, Control, and Dynamics*, vol. 13, pp. 356-362, 1990.

[13] P. R. Grant and L. D. Reid, "Motion washout filter tuning: Rules and requirements," *Journal of Aircraft*, vol. 34, pp. 145-151, 1997.

[14] R. Sivan, J. Ish-Shalom, and J.-K. Huang, "An Optimal Control Approach to the Design of Moving Flight Simulators," *Systems, Man and Cybernetics, IEEE Transactions on*, vol. 12, pp. 818-827, 1982.

[15] G. L. Zacharias, "Motion cue models for pilot-vehicle analysis," DTIC Document1978.

[16] R. Hosman and J. Van der Vaart, *Vestibular models and thresholds of motion perception: Results of tests in a flight simulator*: Delft University of Technology, 1978.

[17] W. Wu and F. M. Cardullo, "Is there an optimum motion cueing algorithm," in *Proceedings of the AIAA Modelling and Simulation Technologies Conference, New Orleans (LA), August 11*, 1997, pp. 23-29.

[18] W. Wu, "Development of Cueing Algorithm for the Control of Simulator Motion Systems,," Master Thesis, State University of New York at Binghamton, 1997.

[19] L. Young and C. Oman, "Model for vestibular adaptation to horizontal rotation," *Aerospace medicine*, vol. 40, pp. 1076-1080, 1969.

[20] J. Meiry and L. Young, "A revised dynamic otolith model," 1968.

[21] J. L. Meiry, "The vestibular system and human dynamic space orientation," 1965.

[22] H. Kwakernaak and R. Sivan, *Linear optimal control systems* vol. 1: Wiley-interscience New York, 1972.

[23] *Rigs of Rods is an open source vehicle simulator based on soft-body physics*. Available: http://www.rigsofrods.com

[24] K. Nelson, T. Black, D. Creighton, and S. Nahavandi, "A simulation-based control interface layer for a high-fidelity anthropomorphic training simulator," in *The Interservice/Industry Training, Simulation & Education Conference (I/ITSEC)*, 2010.

[25] Available: http://www.rigsofrods.com/repository/view/4633